Quenching cross sections for electronic energy transfer reactions between metastable argon atoms and noble gases and small molecules

L. G. Piper, J. E. Velazco, and D. W. Setser
Department of Chemistry, Kansas State University, Manhattan, Kansas 66506
(Received 26 April 1973)

Reaction rate constants for the quenching of electronic energy in metastable argon ($^3P_{0,2}$) by Kr, Xe, and a number of simple molecules have been measured. A hollow, cold-cathode discharge excites the metastables in a flow apparatus. The concentration of metastables was followed by absorption spectroscopy as a function of time and of quenching molecule concentration. Quenching of $Ar^*(^3P_2)$ by Kr, CO, N_2, CF_4, and $H_2(D_2)$ proceeds at rates between 0.6 and 7×10^{-11} cm^3 molecule^{-1} · sec^{-1}. Except for Kr, Xe, N_2, CO, and CH_4, the $^3P_0$ metastable level is quenched slightly more rapidly than the $^3P_2$ level. With the aid of data in the literature, the contribution from the product channels (Penning and associative ionization) are considered for quenching by NO and C_2H_2. These channels appear not to be of major importance for quenching since the ionization efficiency of these two reactions is low: ~ 0.2 for NO and ~ 0.1 for C_2H_2. The quenching mechanism is discussed in terms of both a curve crossing and a "golden rule" rate law; the latter appears to be favored.

I. INTRODUCTION

Electronic energy transfer reactions have received increasing interest over the past few years, since this class of reactions seems to be important in determining the physics and chemistry of the atmospheres of our own and other planets. In addition, electronic energy transfer reactions are extremely important excitation mechanisms in laser systems as in the He–Ne, He–Cd, and Ar–O_2 lasers.[1] Studies undertaken at this laboratory in recent years have focused upon analysis of the product channels from reactions between metastable argon atoms and a variety of small molecules, this analysis being confined to electronically excited product states.[2] In the present work we have undertaken the measurement of the reaction rate constants for the quenching of metastable argon atoms by Kr, Xe, and a variety of small molecules.

The first excited configuration of argon ($3p^5 4s$) results in four states: $4s(\frac{3}{2})_2$ or $^3P_2$, $4s(\frac{3}{2})_1$ or $^3P_1$, $4s'(\frac{1}{2})_0$ or $^3P_0$, and $4s'(\frac{1}{2})_1$ or $^1P_1$. The coupling scheme used is usually j, 1-coupling although we have also included the more familar L–S terminology. These states lie between 11.54 and 11.82 eV above the ground electronic state. Two of these states are metastable [$4s(\frac{3}{2})_2$ and $4s'(\frac{1}{2})_0$] as a result of the electric dipole selection rule, $\Delta J = 0, \pm 1$; $J = 0 \not\rightarrow J = 0$. Recent experiments place the lifetime of these two levels as being greater than 1.3 sec.[3]

We have measured the rate constants for the quenching of both metastable levels. The experimental data presented in this paper along with the information already published from this laboratory provide a large reservoir of data on electronic energy transfer reactions from which models for the reaction mechanism can, hopefully, be constructed.

Until recently, most of the kinetic data available for the quenching of metastable argon atoms was confined largely to destruction of the metastables in pure argon.[4-7] Recently some work has been reported for the quenching of metastable argon by various molecules, but these studies have involved tracer techniques, so that the identity of the precursor of the tracer is open to some speculation.[8,9] In our apparatus, approximately 13% of the total metastable atom concentration is in the $^3P_0$ state, so by implication the tracer studies may be sampling composite rate constants for $^3P_0$ and $^3P_2$. Bourène and LeCalvé, however, saw no evidence for two exponential decay in their oscilloscope traces. The work to be reported here involves direct measurement of the metastable concentration via optical absorption. Our measurements are compared to other reported values in Sec. III B. We discuss some possible mechanisms for quenching in Sec. IV. D.

II. EXPERIMENTAL SECTION

A. Basic Technique

The experiments have been carried out in a discharge flow apparatus. The solution to the kinetic equations for the dependence of the concentration of metastables, [Ar*], as a function of time is

$$\ln[\mathrm{Ar}^*]/[\mathrm{Ar}^*]_0 = -\{D_0/(\Lambda^2[\mathrm{Ar}]) + k_1[\mathrm{Ar}] + k_2[\mathrm{Ar}]^2 + k_Q[\mathrm{Q}]\}\, z/v, \qquad (1)$$

where [Ar] is the concentration of argon carrier gas, D_0 is the diffusion coefficient for metastable atoms in argon, Λ^2 is the characteristic diffusion length, k_1 is the two body deexcitation coefficient

of Ar* in Ar, k_2 is the three body deexcitation coefficient of Ar* in Ar, k_Q is the rate constant for quenching of Ar* by molecule Q, [Q] is the concentration of quenching molecule, and z/v is the length down flow tube (z) divided by flow velocity (v) which gives the observation time.

We have solved the equation for the "plug-flow" approximation and assumed that the metastables are quenched with unit efficiency by collisions with the walls. (Recent experiments have confirmed this assumption.[10]) In general the plug-flow approximation is not valid and requires further refinement. Corrections to this approximation involve multiplying experimentally derived values by a constant, which does not conceptually alter the experimental procedure. This problem will be discussed in more detail in Sec. II. D.

The above equation gives us two options for measuring k_Q, the quantity of primary interest. We can measure pseudo first-order rate constants (making sure that $[Q] > [Ar^*]$), $d\ln[Ar^*]/dz = K$, at fixed total pressure, and at a number of different pressures of quencher. Then a plot of K vs. [Q] will be linear with a slope of k_Q. Alternatively, we can measure the decay constant, $\Gamma = d\ln[Ar^*]/d[Q]$, at a fixed point z. Γ is then equal to $k_Q z/v$. The problem here is in accurately determining z, which when divided by v gives the contact time of the reactants. In general, immediate, uniform mixing at the reagent inlet is not obtained so that z will *not* be the distance from the reagent inlet to the observation point. In order to circumvent this problem, Γ is measured at several different observation points. Then a plot of Γ vs z' (distance from reagent jet to observation point) will yield a straight line whose intercept along the z' axis will be virtual mixing point. The distance from this virtual mixing point to the observation window will then be the value of z used in the determination of k_Q.

We will discuss the procedure for determining k_1, k_2, and D_0 from the decay in pure argon in a later paper. At the present time it is sufficient to note that our results are in general agreement with those in the literature.[4-6]

B. Apparatus

The apparatus has already been described in detail elsewhere,[11] so we will only mention a few of its major points. Argon metastables are produced in a hollow, cold-cathode discharge flow apparatus. The flow tube is 31 mm i.d. and contains a right-angle bend and light trap after the discharge. The metastable concentrations are then measured along the flow tube via absorption of resonance radiation from an Oriel Optics pen lamp. The proper absorption line (811.5 nm for $^3P_2$ and 794.8 nm for $^3P_0$) is selected by a McPherson 0.3 m monochrometer and detected with an RCA 7102 photomultiplier. The light beam is chopped prior to entry into the monochrometer, and the output from the photomultiplier is fed into a PAR HR8 phase sensitive amplifier. The lamp and monochrometer are mounted on an optical rail and can be freely moved parallel to the axis of the flow tube. Most measurements involve single-pass absorption, but in order to boost the absorption signal for the $^3P_0$ measurements, three passes across the tube were usually used (the maximum absorption is only 12% for three passes in $^3P_0$ measurements as compared to 20% for one pass in $^3P_2$ measurements.) The flow rate of argon was measured with a precalibrated Fischer–Porter floating ball flow meter. Reagent flows were measured by monitoring the pressure drop (with a silicon oil manometer) across a calibrated capillary tube. In most cases, reagents were diluted in a 5–10% mixture with argon. The total pressure in the flow tube was measured with a silicon oil manometer.

C. Absorption Measurements

Proper analysis of the experiments requires an accurate absorption law which relates the concentration of metastables to the fractional absorption of the resonance line. The well known Beer–Lambert Law is in general only valid in the limit of small absorptions, depending to some extent upon the ratio of the linewidths of the resonance line to the absorption line. A more accurate, but mathematically more cumbersome absorption law is given by Mitchell and Zemansky as[12]

$$A_\alpha = (I_0 - I)/I_0 = \sum_{n=1}^{\infty} [(-1)^{n+1}(k_0 l)^n/n!\ (1+n\alpha^2)^{1/2}], \tag{2}$$

where n is an integer. α is the ratio of doppler width of the emission line to that of the absorption line. $k_0 l$ is the optical depth of the absorbing species. The optical depth is directly proportional to the concentration of metastables through the relation

$$k_0 l = (2/\Delta\nu_D)(\ln 2/\pi)^{1/2}(\pi e^2/mc)\, Nfl, \tag{3}$$

where N is the density of the absorbing species, f is the oscillator strength of the pertinent transition, m is the electron mass, e is the electron charge, c is the speed of light, and $\Delta\nu_D$ is the Doppler half-width of resonance line given by

$$\Delta\nu_D = [2(2R\ln 2)^{1/2}/c]\ \nu_0\ (T/M)^{1/2}.$$

In general we need not concern ourselves with this exact expression for $k_0 l$ since we are interested only in relative changes of $\ln[Ar^*]$. The determination of α is, however, quite important.

Two approaches that can be used to determine α experimentally are measurement of A_α for several different optical depths, $k_0 l$, or direct determination of the width of the emission line by spectroscopic techniques. The absorption linewidth is calculated assuming pure doppler broadening at room temperature. The normal method for varying optical depth is to compare absorbances for a single pass with those for a multiple pass, i.e., vary l. One has to be very careful in such a study to make sure that the multiple traversals all sample the same section of the reactor. This can be particularly troublesome in a flow apparatus where there is a large radial density gradient across the flow tube. An alternative plan, adopted here, is to maintain the same pathlength, l, but to vary k_0 in a known way. This can be done by comparing absorbance of several different lines all of which are diagnostic of the same species (i.e., vary the f-value of the absorption line). There are four lines in the $4s-4p$ manifold that are particularly useful for absorption measurements on the $4s(\frac{3}{2})_2$ level of argon: $4s(\frac{3}{2})_2-4p(\frac{1}{2})_1$ at 912.3 nm, $4s(\frac{3}{2})_2-4p(\frac{5}{2})_3$ at 811.5 nm, $4s(\frac{3}{2})_2-4p(\frac{5}{2})_2$ at 801.5 nm, and $4s(\frac{3}{2})_2-4p(\frac{3}{2})_2$ at 763.5 nm. There are other lines in the ArI spectrum which terminate at the $4s(\frac{3}{2})_2$ level, but they all have such small oscillator strengths that the measured absorbances would be too small to be accurately determined.

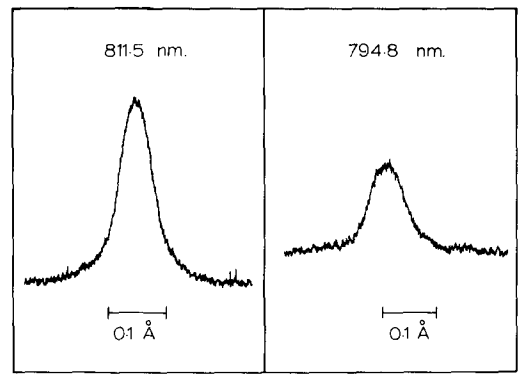

FIG. 2. Photoelectric scan of the 811.5 nm line (diagnostic of the $^3P_2$ level) and the 794.8 nm line (diagnostic of the $^3P_0$ level). The widths, at half-height, of the lines are about 4 and 5 times the room-temperature Doppler widths, respectively. These linewidths are in reasonable accord with the measurements made by varying optical depth since corrections have not been applied for spectrometer resolution and slit function. Notice the absence of self-reversal in the lines.

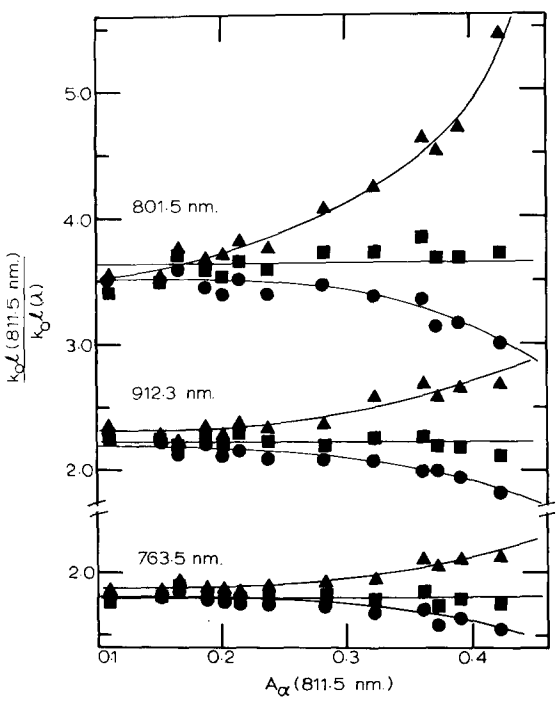

FIG. 1. $k_0 l$ (811.5 nm)/$k_0 l$ (λ) vs A_α (811.5 nm) for three choices of λ diagnostic for the Ar*($^3P_2$) metastable level. Triangles are for $\alpha = 4.0$; squares, $\alpha = 3.5$; circles, $\alpha = 3.0$. The data were fitted until an α was found which gave a reasonably constant ratio of optical depths. The curved lines for cases of $\alpha = 3.0$ and 4.0 are to aid in clarity of presentation only. The horizontal lines through the squares represent the average optical depth ratio over the whole range of metastable concentration. $k_0 l(811.5\ \text{nm})/k_0 l(\lambda) = 3.65$, $\lambda = 801.5$ nm; 2.23, $\lambda = 912.3$ nm; 1.81, $\lambda = 763.5$ nm.

From experimental values of A_α, $k_0 l$ can be determined for an assumed α from Eq. (2). If the proper value of α is chosen, the ratio of optical depths of the 811.5 nm line to that for any of the other three lines should be constant over a range of concentrations [see Eq. (3)]. This constant ratio will then be the ratio of λf for the 811.5 nm line to λf for each of the other lines. In Fig. 1 we have plotted $k_0 l(811.5\ \text{nm})/k_0 l(\lambda)$ versus $A_{\alpha\ell}$ (811.5 nm), where λ is the wavelength of the pertinent transition for three assumed values of α—3.0, 3.5, and 4.0. For the case of $\alpha = 3.5$, the data are seen to be reasonably constant with ratios, $\lambda f(811.5\ \text{nm})/\lambda f(\lambda)$ of 1.81, 3.65, and 2.23 for the 763.5 nm, 801.5 and 912.3 nm transitions, respectively. The absorbance was varied from one point to the next by adding a small amount of oxygen to quench some of the metastables. In order to boost absorption, most of the data were taken with triple-pass conditions. This is important since it is only for high absorbances that differences in α become apparent.

We also had the linewidths measured spectroscopically at the NRC in Ottawa, Canada.[13] We wanted a check for self-reversal and a more direct experimental measurement of the linewidths.

TABLE I. f-values for four lines in the $4s-4p$ array of Ar I.

λ (nm)	(Measured)[a]	(NBS tables)[b]
912.3	0.152	0.159
811.5	0.38	0.51
801.5	0.105	0.092
763.5	0.223	0.239

[a] f-values relative to value of $f=0.38$ derived from lifetime measurement of Ref. 16.

[b] Reference 15.

Figure 2 shows the results of the measurements of two such lines. There is no self-reversal. The widths at half-height for these lines are between four and five times the doppler width at room temperature, in reasonable accord with our other experimental determinations. Lack of knowledge of the spectrometer slit function precludes a detailed analysis of the spectroscopically measured linewidths. In the experiments to measure rate constants, we cooled our lamps by conduction to ~ 100 °K in order to make the emission line more narrow, hoping thereby to reduce the value of α. The spectroscopic measurements indicated, however, that the change in linewidth upon cooling was negligible. The greater-than-doppler width of the line and its small change with temperature indicates that effects other than doppler broadening determine the width of the emission line. In view of the large polarizability of Ar*,[14] the broadening presumably is caused by various collisional processes.

With accurate linewidth information in hand, we tried to find a suitable substitute for the absorption law given above which would be more mathematically tractable. A modified form of the Beer-Lambert Law, $I=I_0\exp\{-a(k_0l)^\gamma\}$ gives $\ln(\mathrm{Ar}^*) \propto -\ln\ln(I_0/I) \propto \ln(k_0l)$. Plotting $-\ln\ln(I_0/I)$ vs. $\ln(k_0l)$, where the values for k_0l are taken from the more accurate absorption law (2), gives good linearity up to absorbances of 30%. The slope of this line, γ, is 0.95, only slightly different from the pure Beer-Lambert case. We used this modified absorption law in our computer analysis of the data.

As outlined above, we also have determined the relative oscillator strengths for the lines under consideration. A recent publication by the NBS lists the oscillator strengths for these and a number of other lines.[15] Our relative oscillator strengths agree with the published values to within 10% (see Table I) for all save the line at 811.5 nm, which is, unfortunately, the one of most interest. Our values have been normalized to an oscillator strength of 0.38 for the 811.5 nm line as derived from a recent lifetime measurement.[16] This is in contrast to the value of 0.51 published in the NBS tables. The reasons for this discrepancy are unknown, although the authors of the NBS tables admit that the published values for oscillator strengths tend to fall into two groups, differing from each other by about 30%.

Knowing the oscillator strengths of the absorption lines and the line width parameter α, we can calculate the density of metastables in the flow tube, using Eq. (3). At an absorption of 20%, near the maximum observed in the runs, the density of metastables in the $^3P_2$ level is 2.5×10^{10} atoms/cm^3. For the $^3P_0$ level, the maximum absorption for a single pass is 4% which results in a density of 2.6×10^9 atoms/cm^3 in the flow tube. In our earlier studies[2] in which the reagent flow was mixed concentrically with the Ar* flow and shorter decay times separated the discharge from the mixing zone, the concentrations were 2-3 times higher,

D. Flow Analysis

The analysis of the relevant flow equations for cases involving laminar flow and unit deactivation of the species of interest at the walls has been thoroughly considered in the literature.[17-23] In general, the gas flowing into the flow tube will relax into a fully developed laminar flow with a parabolic velocity profile after a time which is dependent upon the Reynolds number, R, describing the flow and tube geometry. This time is usually translated into a traversal distance $d=0.227\,aR$ [17] through which the gas must flow before fully developed parabolic flow exists in the tube (a is the flow tube radius). In our experiments R typically ranges between 60 and 100, which gives a value of d between 20 and 35 cm. The flow will be in transition between plug and parabolic flow between the point of entry of carrier gas into the flow tube and this distance d. If all measurements are made after development of parabolic flow, the measured rate constants, under the assumption of plug flow, should be multiplied by a factor of 1.6 to give the value of the rate constant under parabolic-flow conditions. This factor of 1.6 only holds if axial diffusion is negligible, and if the reagent is uniformly dispersed at the mixing point without perturbations from inlet effects. We have also neglected contributions from slip and axial velocity gradients which are negligible under our experimental conditions.

This parabolic-flow model is not quite applicable in the present case so that full corrections to the plug-flow rate constants are not justified. One problem arises in deciding at what point fully developed parabolic flow has been achieved. Our apparatus[11] introduced perturbations into the flow

pattern at the right-angle bend after the discharge, and at the reagent inlet. We cannot achieve suitable absorptions for distances away from the reagent inlet which satisfy the full relaxation to parabolic flow, although that would be the best approach. Since our measurements are therefore made along some intermediate region where the gas is relaxing toward parabolic flow, some intermediate correction to the plug-flow model seems to be in order. On this basis a factor of 1.3 seems reasonable.[24]

A further problem arises in the determination of the perturbations to the solutions of the flow equation which are introduced by inlet effects. In the review by Ferguson *et al.*[17] this problem has been considered for two different geometries, ideal point source and coaxial cylinder. In both instances, the necessary correction is in such a direction as to reduce the original factor of 1.6. The correction is sufficiently severe that the correction factor to the plug-flow rate constant could conceivably be less than unity. Our "shower head" reagent jet should provide better mixing and less perturbation to the radial distribution of metastables than does either an ideal point source or a coaxial cylinder. Still, there should be enough perturbation from the assembly that a significant correction should be applied. A further problem is that our measurement for concentration is for some average across the flow tube, rather than a axial measurement of the concentration. For these reasons, we have further reduced the adjusted correction factor of 1.3 to a final value of 1.15. We believe that this procedure gives rate constants with an absolute uncertainty of ±20%.

III. EXPERIMENTAL RESULTS

A. Presentation of Data

Figures 3–8 show plots of typical data. Figures 3–5 and 8 are plots from the first method outlined in Sec. II. A for the pseudo-first-order measurements. The fixed point procedure is demonstrated by Figs. 6 and 7. In most instances, we measured the decay constant, Γ, at only two points, but the straight line extrapolation generally gave consistent results for the virtual mixing point, typically −5 to −8 cm. If the intercept did not fall within this range, the experiments were checked. Slight differences in the intercept are expected since different reagents will take varying amounts of time to completely diffuse across the flow tube. The negative intercept is a result of inlet effects.

The results of the experiments are listed in Table II. In most cases only one measurement of the rate constant was made at a pressure near 1 torr. Studies with H_2 (1.06 to 2.52 torr) and N_2 (0.71 to 1.54 torr) indicated a constancy in rate constant with pressure within experimental error.[11] For some cases, we measured the quenching rate constant at 1 torr several times, and in all instances the measured values agreed to within ±10%. In the case of N_2 and CO, we also checked our measurements by following the decay of emission[23]

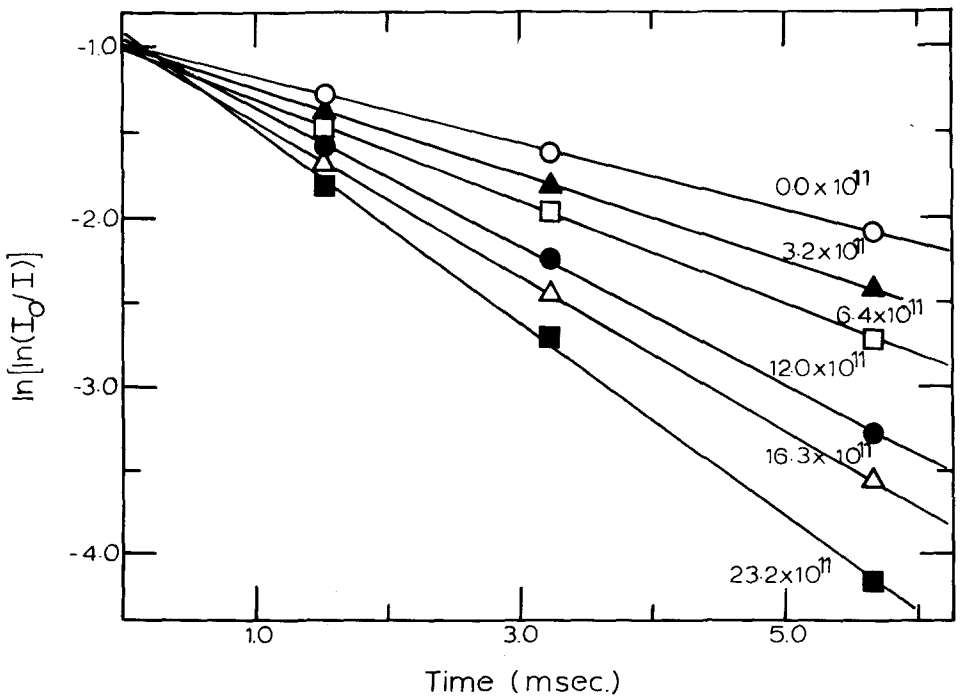

FIG. 3. The decay of $Ar^*(^3P_2)$ metastable concentration as a function of time and of Xe concentration. The slopes of the lines, measured at the fixed concentration (molecule/cm^3) listed by each line, are the pseudo first-order rate constants. The total pressure was 1.06 torr, and the flow speed was 4.2×10^3 cm sec^{-1}.

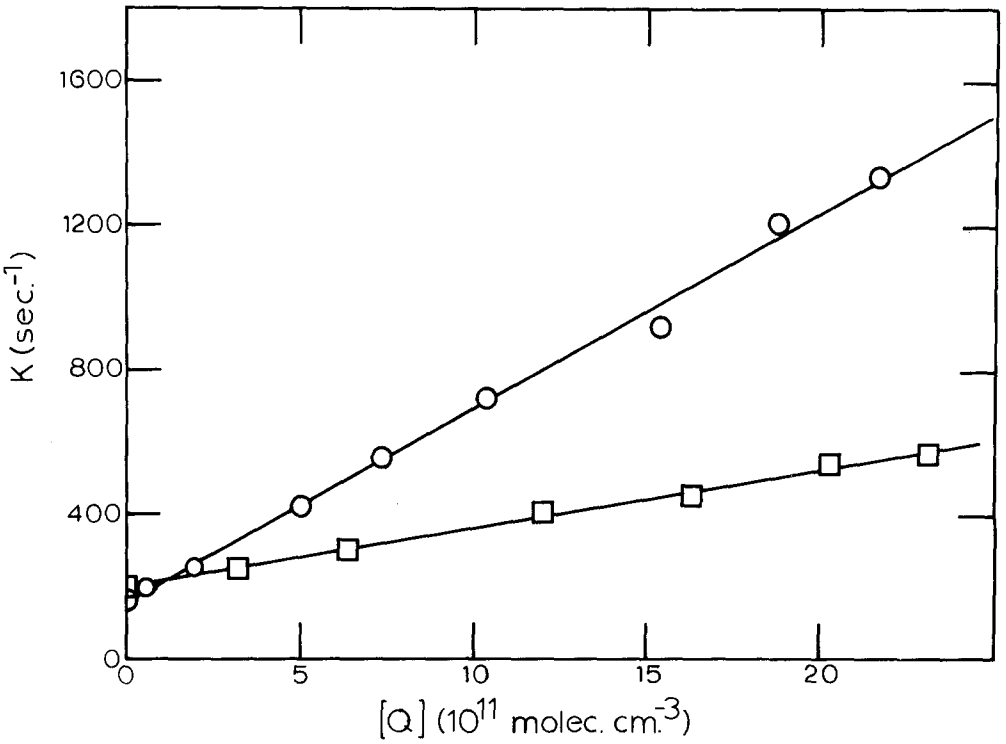

FIG. 4. The pseudo first-order rate constant as a function of concentration for quenching of $Ar^*(^3P_2)$ by Xe (squares) and HCN (circles). The slopes of the lines give the quenching rate constants.

from N_2^* and CO* as a function of time and of reagent concentration. This method cannot differentiate between the two metastable levels, so the measured rate constant should be some average of the individual rate constants for quenching of the two species; although since the $^3P_2$ level accounts for ~90% of the total ^3P metastable concentration, the rate constants as measured in emission ought to compare well with the $^3P_2$ constants. Our emission values were lower than the measured values of the quenching rate constants for the $^3P_2$ level as measured by absorption, but agree within 20%, and therefore the agreement is satisfactory. A slightly lower rate constant from emission measurements would be expected in the case of N_2, as the $^3P_0$ level is quenched by N_2 with about half of the efficiency for quenching the $^3P_2$ level (see Fig. 5). This is not the case for CO, because $^3P_0$ rate constant is higher than that for $^3P_2$. It is possible that the $^3P_0$ state of argon excites different emissions in CO than $^3P_2$ and, that the ones we observed (~360 nm) were excited by $^3P_2$. The specific product channels for CO with the different argon states have not been thoroughly studied,[2e] but the large difference in cross sections implies different product channels. Finally, we checked the rate constants for N_2 and CO, using the emission technique, but in a different apparatus, which had a much slower pumping speed and more inherent sources of error. Still, agreement with the absorption values was good, being within 40% for CO and 10% for N_2. We are therefore confident in the values reported.

All of the listed values have been obtained by least squares fit to the data. The scatter in the data points for the $^3P_2$ measurements is better than 4% in all cases except for the hydrocarbons, COS, and CS_2. Perhaps a better measure of the error in the method is the reproducibility of the measurements from one day to another. As mentioned above, this reproducibility was better than 10%. Thus the relative reliability of the data is consid-

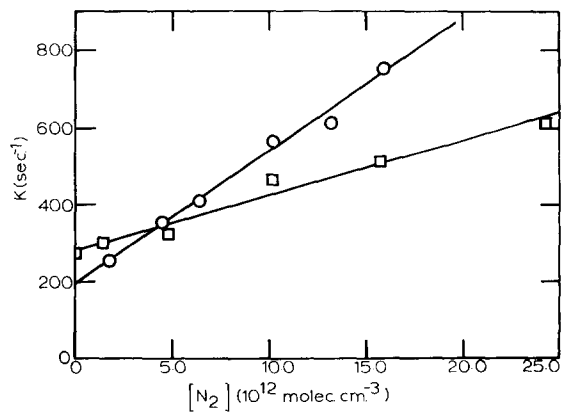

FIG. 5. Pseudo first-order rate constant vs N_2 concentration for quenching of $Ar^*(^3P_2)$ (circles) and $Ar^*(^3P_0)$ (squares).

TABLE II. Metastable argon quenching rate constants and cross sections.[a]

Quenching molecule	Ar*($^3P_2$)		σ_Q[b]	Ar*($^3P_0$)		σ_Q[b]	Literature	
	k_Q	σ_Q(Å^2)	$\overline{\sigma_{HS}}$	k_Q	σ_Q(Å^2)	$\overline{\sigma_{HS}}$	k_Q(Ar*$^3P_{0,2}$)	σ_Q(Å^2)
Kr	0.62	1.3	0.014	0.23	0.48	0.005	1.4	2.9[c]
								1[d]
								~2[e]
Xe	18	40	0.37	30	58	0.54	21	46[c]
H_2	6.6	3.6	0.043	7.8	4.3	0.051	11	6.0[c]
								0.3[d]
D_2	4.7	3.6	0.043	7.8	5.9		8.3	6.3[c]
N_2	3.6	5.8	0.06	1.6	2.5	0.026	2.9	5.0[c]
							3	5.2[f]
							2.8	4.5[g]
								~6[h]
CO	1.4	2.3	0.024	13	21	0.22	5.5	8.9[c]
							1.5	2.4[g]
O_2	21	35	0.38	24	41	0.44	18	29[c]
							12	21[g]
								~20[i]
								35 ±4[j]
NO	22	36	0.39	25	41	0.44	17	26[c]
Cl_2	47	95	0.90					
HCl	35	61	0.68					
HBr	72	150	1.55					
HI	70	155	1.49					
HCN	58	94	0.92					
BrCN	46	100	0.83					
N_2O	44	81	0.81	48	87	0.88	43	80[c]
CO_2	53	97	0.96	59	108	1.07	56	100[c]
COS	79	155	1.48				70	140[c]
CS_2	106	218	1.98				100	200[c]
SF_6	16	36	0.28	17	38	0.29	40	90[c]
CF_4	4	8	0.07	4	8	0.07		
CHF_3	31	64	0.58					
CH_4	33	45	0.46	55	74	0.75	60	81[c]
C_2H_6	66	109	1.00				73	120[c]
C_3H_8	73	134	1.07				80	150[c]
n-C_4H_{10}	76	149	1.08				89	175[c]
i-C_4H_{10}	71	138	1.00					
C_2H_2	56	89	0.86				47	74[c]

[a] k_Q has units of 10^{-11} cm^3 molecule^{-1} sec^{-1}; $\sigma_Q = k_Q/\bar{v} = [8kT/\pi\mu]^{1/2}$, the mean Boltzmann speed.

[b] $\sigma_{HS} = \pi R_c^2$, $R_c = \frac{1}{2}(\sigma_{Ar^*} + \sigma_Q)$ with $\sigma_{Ar^*} = 7.4$ Å, see text.

[c] Reference 8.

[d] Reference 4.

[e] O. P. Bochkova, Opt. and Spectrosc. **28**, 88 (1970).

[f] J. M. Calo and R. C. Axtman, J. Chem. Phys. **54**, 4961 (1971).

[g] Reference 9.

[h] H. A. Schultz, J. Chem. Phys. **44**, 377 (1966).

[i] Reference 47.

[j] M. E. Gersh and E. E. Muschlitz, Jr. submitted to J. Chem. Phys., 1973. Their measured Ar*($^3P_{0,2}$) composite cross section is listed in the table. They measured $\sigma_Q(^3P_2) = 33.5 \pm 5$ Å^2 and $\sigma_Q(^3P_0) = 44 \pm 9$ Å^2 in a molecular beam apparatus.

ered to be ±10%, except in the cases noted, with a further uncertainty in the absolute values of the measurements of ±20% due to flow considerations.

The $^3P_0$ measurements, primarily taken by the fixed-point technique, had a scatter of up to 10% in the least squares fits to the plots of $\ln\ln(I_0/I)$ vs [Q]. There is the additional uncertainty in the virtual point of mixing which gives up to an additional 10% uncertainty in the rate constant. Thus the total uncertainty in the relative values of the $^3P_0$ data is ±15%.

The hydrocarbons, COS, and CS_2 introduced the experimental problem of the reagents dissolving in the stopcock grease and in the oil of the manom-

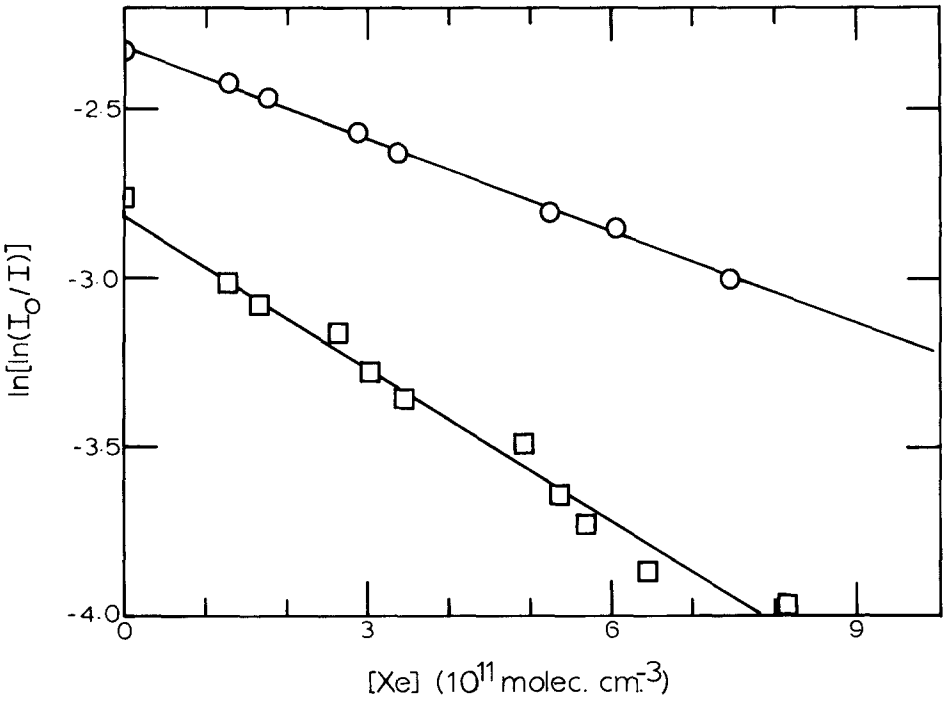

FIG. 6. The decay of $Ar^*(^3P_0)$ as a function of Xe concentration at distances of 13.4 cm (circles) and 26.8 cm (squares) from the reagent inlet. These measurements were made under triple-pass conditions for a bulk flow speed of 6.4×10^3 cm sec^{-1} and pressure of 1.02 torr. The slopes of these lines give the decay constant, Γ, for the two different observation points.

eter used to measure reagent flows. This affects the data in two ways. The reagent concentrations in the Ar–Q reagent mixture will be depleted by dissolving in the grease and oil, resulting in an overestimation of the reagent concentration. In addition, the density of the oil in the flow meter will change resulting in an erroneous reading (too high) of the pressure drop across the capillary. This also causes overestimation of the reagent concentrations. The data showed uniform curvature indicative of this problem (see Fig. 8). These rate constants are derived by taking a limiting straight line slope to the low reagent concentration points in the plot of K vs Q. This procedure should give relative uncertainties for these gases of ~20%.

B. Comparison with Other Studies

The agreement between our rate constant values and those of Bourène and LeCalvé[8] is quite good,

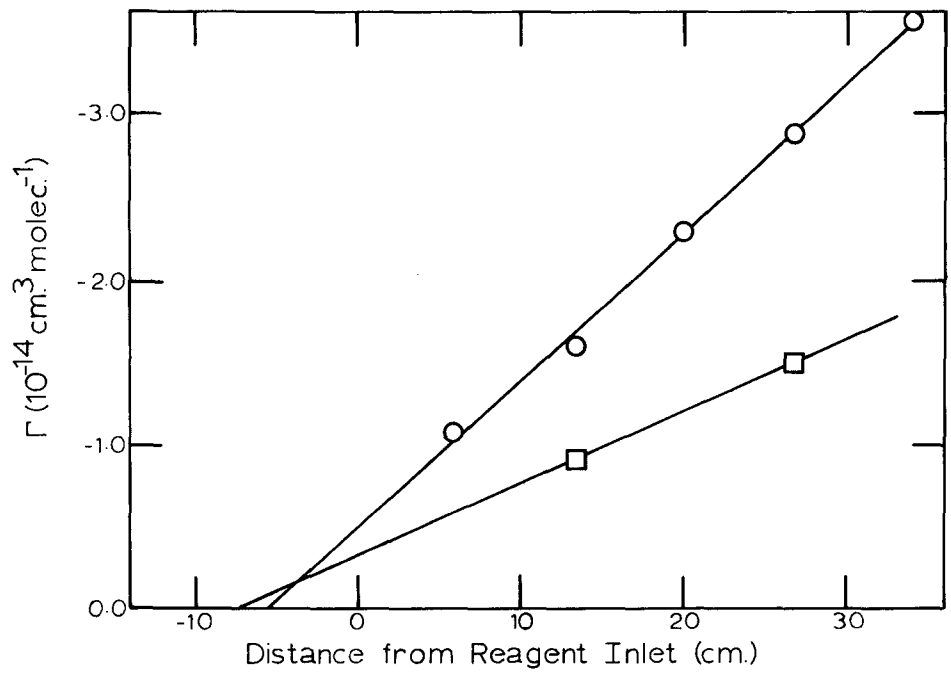

FIG. 7. The decay constant, Γ, as a function of distance from reagent inlet for $Ar^*(^3P_2)$ + Kr (circles) and $Ar^*(^3P_0)$ + Xe (squares). The intercept gives the virtual point of mixing, and the contact time of the reactants is taken to be the distance from the virtual point of mixing to the observation point divided by the bulk flow velocity. The quenching rate constant is computed by dividing Γ by the contact time.

see Table II, except for $H_2(D_2)$, CO, SF_6, and Kr. In the case of SF_6, Bourène and LeCalvé note that they had trouble due to the large electron capture cross section of that gas. Our CO rate constant agrees quite well with the value given by Gutcheck and Zipf.[9] In addition, the emission studies with two different apparatuses confirm our own value. The value of Bourène and LeCalvé lies between the values we have measured for the $^3P_2$ and $^3P_0$ levels of Ar. It is conceivable that the $^3P_0$ concentration makes up a larger fraction of the total metastable density following their excitation pulse than that observed in our apparatus, although, as noted, Bourène and LeCalvé only saw single exponential decay. The discrepancy in the case of Kr is unknown; although, N_2, Bourène and LeCalvé's tracer, is a vastly more efficient quencher of Ar* than is Kr, and might therefore have interfered with their measurements. Our rate constant for quenching of Ar* by Kr coincides with the value of Phelps and Molnar[4] who also used an absorption technique. The discrepency in the case of $H_2(D_2)$ is unknown although the values lie just within the combined experimental uncertainties of the two methods.

No other measurements have been made of the quenching of the $^3P_0$ level, thus, no comparisons can be made. In most instances the upper metastable, is quenched with only a slightly greater efficiency. Exceptions to this are Kr, Xe, N_2, CO, and CH_4.

For purposes of comparison, we have also listed the hard sphere quenching efficiency for these reactions. Hirschfelder and Eliason[25] have calculated that the hard sphere collision diameter of Ar

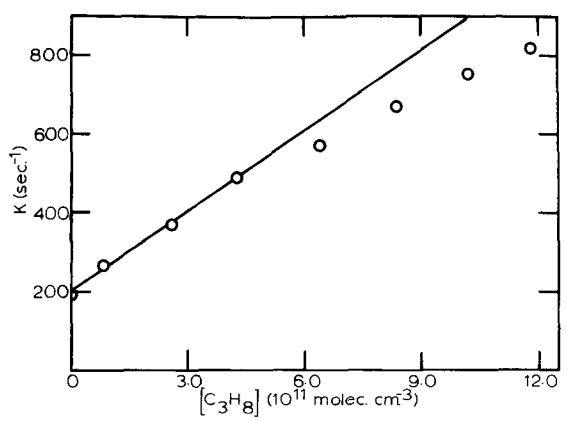

FIG. 8. The pseudo first-order rate constant as a function of C_3H_8 concentration for quenching of $Ar^*(^3P_2)$. The deviation from linearity at higher reagent concentrations is taken as a sign of absorption of C_3H_8 in stopcock grease and manometer oil (see text). The quenching rate constant is taken to be the limiting straight line fit to the data points.

in its 4s states is ~9.8 Å. This value is based on a rule of thumb whereby the collision diameter is equal to $2r+1.8$, where r is the atomic radius. In light of more recent calculations, the value used for the atomic radius is probably ~30% too large.[26a] Therefore the atomic radius of Ar*, as calculated by Hirschfelder and Eliason was decreased by 30% and a value of 7.4 Å was used for the collision diameter.[26b] The hard sphere collision cross section was calculated by standard methods, $\sigma_{HS}=\pi R_c^2$ where $R_c=\frac{1}{2}(\sigma_{Ar}{}^*+\sigma_Q)$.[27] That Ar* will have a larger orbital radius than ground state Ar is reflected in the diffusion coefficients of the two species in Ar. Metastable argon has a diffusion coefficient in argon of 1.7×10^{18} $cm^{-1}\cdot sec^{-1}$ [4-6] as opposed to the self diffusion coefficient of ground state argon 5.0×10^{18} cm^{-1}, sec^{-1}.[27] For a Lennard-Jones potential, based upon C_6 as calculated from the Slater–Kirkwood approximation and then increased 10% to account for higher order effects, and a $\sigma_{Ar}{}^*=7.4$ Å, the calculated coefficient of diffusion[27] of Ar* is 2.8×10^{18} $cm^{-1}\cdot sec^{-1}$, in modest accord with the experimantal value for that quantity. Thus the choice for σAr^* is slightly higher than that for K (~6 Å), which is expected since the orbital radius also is reflected in the larger polarizability for Ar* than for potassium.[14,28] For this choice of a collision diameter, the efficient gases quench the metastable atoms in less than three collisions.

IV. DISCUSSION

In our previous work we have identified many of the exit channels for these quenching processes. A summary was presented in Ref. 11. Even for quenching molecules with $I < 11.7$ eV, a large amount of neutral dissociative excitation was found; furthermore, there is no abrupt increase in cross section when Penning or associative ionization becomes a possible exit channel. In Sec. I the relative role of Penning and associative ionization versus other product channels for two simple cases, the quenching by NO and C_2H_2, will be examined (see Table III). Following that several recently published papers that have some related concerns to the work at hand will be considered. In order to understand the quenching of metastable states, some of the recent studies of the quenching of argon resonance states[29] will be examined. Finally we attempt to relate our data to several of the quenching mechanisms which have been proposed in the literature.

A. Penning and Associative Ionization for NO and C_2H_2

Holcombe and Lampe have recently studied associative ionization for ^3P metastables with NO or C_2H_2.[30] They measured the product of the associa-

tive ionization rate constant for the metastable-molecule collision and the cross section for electron impact excitation of Ar to the metastable levels at an electron energy of 22 eV. Using the pioneering work of Herman and Cermak[31] and results of Hotop, [32] they deduced the product of the total ionization rate constant (both Penning and associative ionization) and the electron excitation cross section, which is 1.8×10^{-27} cm^5 sec^{-1} for NO and 2.8×10^{-27} cm^5 sec^{-1} for C_2H_2. Further analysis was impossible since the excitation cross sections were not known.

Winicur and Knuth[33] have published absolute cross sections for the excitation of Ar to the $4s\,^3P$ metastable levels over the energy range of 60–100 eV. We hoped, initially, to use their values to place the relative electron excitation cross sections of Lloyd *et al.*[34] on an absolute basis so that the excitation cross section at 22 eV could be found. We could then derive the rate constant for formation of ions and combine these values with our total quenching rate constants to obtain the ionization efficiency for the quenching by NO and C_2H_2. Unfortunately, the published cross sections of Winicur and Knuth seem to be unusually large, and the energy dependence is opposite to what is expected based on the work of Lloyd *et al.* and Born approximation calculations.[35]

We have tried to resolve this problem in an alternative fashion. Peterson and Allen[36] report a list of parameters which can be used to give electron excitation cross sections into any specific argon energy level as a function of energy. Metastable formation is primarily through cascade from higher levels. Consequently, the total composite electron excitation cross section was calculated at 22 eV for all excited states of neutral argon, except the 4*s* resonance states, to be ~ 8×10^{-17} cm^2. If half of these excited states cascade into ^3P metastable levels, the ^3P metastable excitation cross section will be ~ 4×10^{-17} cm^2. This value in conjunction with the results of Holcombe and Lampe gives ionization rate constants of 4.5×10^{-11} and 7×10^{-11} cm^3 sec^{-1} for NO and C_2H_2, respectively, which lead to ionization efficiencies of the quenching reactions of 0.2 for NO and 0.1 for C_2H_2. Thus Penning ionization and associative ionization are only minor channels in the quenching of Ar* by NO and C_2H_2. This estimate of the ionization efficiency of the $^3P_{0,2}$ levels is in agreement with that given by Clark *et al.*[37] for the ionization efficiency of $^3P_1$ argon with NO (0.2), but in poor agreement with the value of 0.47 given by Klots,[38] also for the $^3P_1$ level. In both cases the total quenching rate constants agree within experimental error (see below) although Clark *et al.* arrived at their rate constant on the dubious assumption that excited argon atoms have the same collision diameter as ground state argon. This assumption does not affect the ionization efficiency factor, however. The ionization efficiency deduced for the metastable states with C_2H_2 also disagrees with Klots' $^3P_1$ data, since he obtained a value of 0.85.

Zapesochnyi and Feltsan have measured electron excitation cross sections for the 4*p* levels of argon.[39] As these levels cascade to the 4*s* levels, an excitation cross section for the two metastable levels can be calculated with the aid of branching ratios[15] for the 4*p*–4*s* transitions. The calculated value of the ^3P metastable excitation cross section at 22 eV is ~7×10^{-17} cm^2 based on this method. However, some of the excitation cross sections have been corrected for cascade while others have not, so the reliability of this calculation is subject to some skepticism. In addition, energy loss spectra indicate that the actual cross sections are probably smaller than those reported by Zapesochnyi and Feltsan.[36] It is encouraging, however, that the value reported by these two workers is within a factor of 2 of our estimate, and casts further doubt on the magnitude of the values reported by Winicur and Knuth. The effect of using larger excitation cross sections, such as those of Winicur and Knuth, is to further reduce the ionization efficiencies.

We conclude for both NO and C_2H_2 that ionization is only a fraction of the total quenching pathways. This conclusion is in agreement with earlier[8,11] deductions about the lack of change in quenching cross sections when $IP < 11.7$ eV and for the strong emission from neutral products in those reactions. Further work with NO and C_2H_2 is needed to identify other exit channels.

B. Related Studies

Parks *et al.*[40] in their development of an "energy pathways" model have assumed that the Jesse effect in argon arises primarily from sensitized ionization of the impurity by the $^1P_1$ level of argon. The Jesse effect is the enhanced ionization in a gas, which is being bombarded by high energy particles, upon the introduction of small amounts of an impurity gas whose ionization potential is lower in energy than the excited states of the neutral host gas. They[40] assume that the energy trans fer cross section from the $^1P_1$ level is much greater than from either the $^3P_2$ level or from excited states of molecular argon. Rate constants for quenching by C_2H_2 and C_2H_4 of 1.1×10^{-9} and 6.5×10^{-10} cm^2 molecule$^{-1}\cdot$sec^{-1}, respectively, are quoted. These numbers can be compared with our rate constant for quenching the $^3P_2$ level by

C_2H_2 of 5.6×10^{-10} cm^3 molecule$^{-1}\cdot$sec^{-1} and the ^3P metastable quenching rate constant by C_2H_4 of 6.4×10^{-10} cm^3 molecule$^{-1}\cdot$sec^{-1} as measured by Bourêne and LeCalvé.[6] Clearly the metastable quenching rate constants are not negligible in comparison to the resonance state quenching rate constants, although the ionization efficiencies for the two quenching processes could differ. The difference discussed above in ionization efficiency (0.84 vs ~0.1 for C_2H_2) together with the differences in the quenching rate constants would make an order of magnitude difference in the ionization production efficiencies with C_2H_2 for the Ar species. A significant difference in the populations of the two excited species, which may be the case since excitation by high energy particles generally follows the oscillator strength of the excitation transition (unlike low energy electrons[41]), might further add to the disparity in ion production. However, it is also possible that the relative ionization efficiencies of the two species may not differ as widely as that suggested above for C_2H_2, or that cascade or collisional processes do significantly populate the ^3P metastable levels. Clearly further studies are in order before the Jesse effect in argon can be understood.

Gedanken *et al.*[42] have studied electronic energy transfer between excited rate gas atoms and molecules with other rare gases. Their published cross sections for the transfer of energy from excited argon atoms to Xe and Kr are 2300 and 59 Å^2, respectively. The Ar($^1P_1$) level was considered as the main energy carrier. Comparison of our measured $^3P_2$ quenching rate constants with those of Klots for the $^1P_1$ level in collisions with NO and several hydrocarbons (see below) indicates that the $^1P_1$ level is, in general, less than a factor of two more efficient in transferring electronic energy than is the $^3P_2$ level. Gedanken *et al.* suggest that their measured cross sections are only order of magnitude estimates because of the uncertain lifetimes of the excited molecules. However, based on their kinetic analysis, this lifetime dependence only affects the molecular quenching rate constant and not the excited atom quenching rate constant. A difference of a factor of 50 between the resonance and metastable quenching rates is somewhat suspect.

TABLE III. Ionization efficiency in excited argon interactions with NO and C_2H_2.

Molecule	Ar*($^3P_{0,2}$)[a]	Ar*($^3P_1$)
NO	0.2	0.2[b]
		0.47[c]
C_2H_2	0.1	0.85[c]
		0.76[d]

[a] Based on a combination of our measurements with those of Refs. 30 and 36 (see text).
[b] Reference 37.
[c] Reference 38.
[d] R. L. Platzman J. Phys. Rad. 21, 853 (1960).

TABLE IV. Comparison of metastable and resonance state argon quenching rate constants.[a]

Quenching molecule	Ar($^3P_2$)	Ar($^3P_0$)	Ar($^3P_1$)	Ar($^1P_1$)
H_2	0.66	0.78	0.95[b]	0.062[b]
D_2	0.47	0.78	0.22[b]	0.39[b]
NO	2.2	2.5	2.0[c]	6.0
O_2	2.1	2.4	0.09[d]	
N_2	0.36	0.16	0.06[d]	
C_2H_2	5.6		4.6[c]	8.7[c]
C_2H_6	6.6		6.2[c]	10.7[c]
C_3H_8	7.3		6.25[c]	10.7[c]
n-C_4H_{10}	7.6		6.6[c]	11.9[c]
i-C_4H_{10}	7.1		6.1[c]	11.0[c]

[a] Units of k_Q are 10^{-10} cm^3 molecule$^{-1}\cdot$sec^{-1}.
[b] Reference 43, absolute values were obtained by setting the cross section for quenching by HD equal to that predicted by dipole–dipole theory.
[c] Reference 38.
[d] These values are reported in Ref. 37 relative to k_0 for NO; we have used the k_Q(NO) value from Ref. 38 to obtain absolute values of the rate constants.

C. Comparison with Studies of Resonance States

Three recent studies on argon resonance state quenching have appeared: Klots investigated the quenching and sensitized ionization efficiencies of the $^3P_1$ and $^1P_1$ levels of argon with NO and a number of hydrocarbons[38]; Clark *et al.*[37] explored the quenching of the $^3P_1$ level by N_2, O_2, and NO, and ionization efficiencies for NO and O_2 ($^1\Delta_g$); Fink *et al.*[43] measured the partitioning of energy into the various product states from the quenching of both argon resonance states by H_2, D_2, and HD. Table IV gives a comparison of quenching rate constants for the metastable and resonance states. The values of Clark *et al.* for N_2 and O_2 were measured relative to the value for NO, which previously was measured[44] in their laboratory as 4×10^{-10} cm^3 molecules$^{-1}\cdot$sec^{-1}. On the basis of hard sphere considerations, however, they favor a $k_{NO}=1.6\times10^{-10}$ ml molecule$^{-1}\cdot$sec^{-1}. We scaled their values using Klots' Ar* ($^3P_1$) quenching rate constant for NO. Fink *et al.* placed their relative quenching cross sections for formation of given vibrational–rotational hydrogen states on an absolute basis by normalizing their strongest observed excitations to the value predicted by the long range dipolar quenching theory.[43,45]

The values for the $^3P_2$ level quenched by hydro-

carbons are surprisingly close to the $^3P_1$ results of Klots. Klots' $^1P_1$ rate constants are about a factor of 1.5 greater than our numbers for Ar ($^3P_2$). This is nearly the ratio of the oscillator strengths of the $^1P_1$–$^1S_0$ to $^3P_1$–$^1S_0$ transitions taken to the $\frac{2}{5}$ power (1.7), which is that expected from the dipole–dipole coupling model. Note also that the ratio of the rate constants for quenching the $^3P_0$ level to the $^3P_2$ level by CH_4 is 1.7. Furthermore, Klots' data, with the exception of NO, correlates with the optical dipole coupling model of Watanabe and Katsuura.[46] Since the metastable $^3P_2$ level has no allowed dipole transition, it is very surprising that the rate constants are equally large as for Ar ($^3P_1$). This is discussed in more detail in Sec. IV. D.

The rate constant for quenching Ar* ($^3P_1$) by H_2 agrees to within about 30% with our own number for the $^3P_2$ level of argon, and their value for D_2 differs from ours for both metastable levels by only a factor of 2. This seems a rather good coincidence considering that the exit channels for quenching the metastable state and the resonance state are different. Excitation by the metastable levels populates the $a\ ^3\Sigma_g^+$ state, which leads to the hydrogen blue continuum, whereas the resonance levels populate the $B\ ^1\Sigma_u^+$ state of hydrogen.

In light of the similarity with Klots, the difference between our $^3P_2$ quenching rate constants for N_2 and O_2 and those[37] for quenching of the $^3P_1$ level is surprising. This disparity is particularly difficult to rationalize since the $^3P_0$ level of argon is quenched by O_2 with just slightly greater efficiency than the $^3P_2$ level, and N_2 quenches the upper metastable with about half the efficiency with which it quenches the lower metastable. As the $^3P_1$ resonance state lies between the two metastable levels in energy, we cannot understand why the resonance level is quenched so much more slowly than the two metastable levels. Bennett *et al.*[47] indicate that the argon resonance levels and metastable levels are quenched by oxygen with about equal efficiency.

D. Discussion of Quenching Mechanisms

The data listed in Table II can be divided into two groups on the basis of the magnitude of the quenching cross section. Weak quenchers, including Kr, N_2, CO, $H_2(D_2)$, and CF_4 all have quenching cross sections less than 10 Å^2, whereas, the rest of the molecules have quenching cross sections in excess of 35 Å^2 and therefore can be considered as strong quenchers. This division might indicate in a general way that several different mechanisms must be considered for the quenching process. In addition, the estimation that ionization channels are only of minor importance in the quenching of metastable argon by NO and C_2H_2 would also indicate, that even for a given quenching molecule, several different quenching mechanisms should be considered.

Several models have appeared in the literature which purport to lay theoretical basis for quenching reactions.[2a,42,43,46,48–54] Earl *et al.*[49] have studied the quenching of Na* ($3p^2P$) by several different gases over a range of velocities. They have invoked the model, previously used by Bell, *et al.*[55a] in their description of Penning ionization by He metastables, whereby quenching occurs for those collisions whose trajectories penetrate (with a probability w) the centrifugal barrier of the effective potential. At a given temperature, and under the assumption of constant w, the quenching cross section, according to this model, will vary as $C_6^{1/3}$, where C_6 is the van der Waals coefficient. We tested this model by plotting the quenching cross section vs C_6[55b] on a log–log plot (see Fig. 9). If this model were valid for our data, the plot should have a $\frac{1}{3}$rd slope, but it does not. There is, however, a strong correlation and a unit slope fits nearly all data points. Neither does this model seem to hold for He metastable quenching cross sections[56,57] which are plotted in the same manner in Fig. 10. The problem may lie in the fact that w is not constant as indicated by the fact that hard sphere efficiencies vary between 0.03 to 1 for the gases that have been studied.[57] This being the case, the model is not particularly useful so we will not consider it further.

We can discuss a curve crossing model[2a,43,58] with reference to Fig. 11. The input channel,

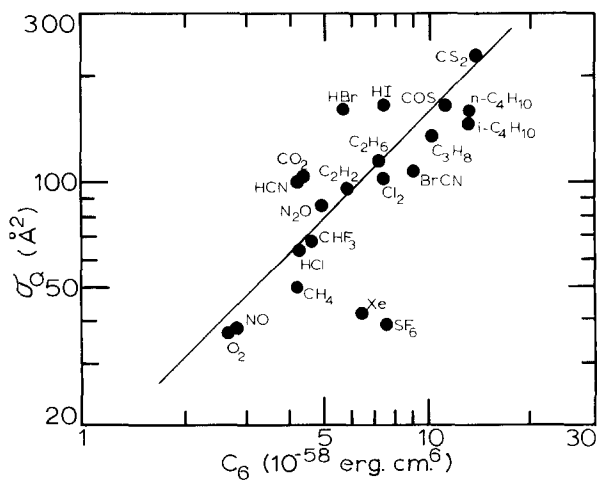

FIG. 9. Ar*($^3P_2$) metastable quenching cross sections plotted against C_6, the van der Waals dispersion parameter. C_6 was calculated from the Slater–Kirkwood approximation; induction terms were not added. The reference line is of unit slope.

Ar^*-Q is essentially flat until repulsion begins to set in at ~ 6Å (see above, Sec. IIIB). In general, the ratio of collision diameters of excited to ground state species will be larger for atoms than for molecules, except in the case of molecular Rydberg states. Thus the repulsive wall of the Ar^0-Q^* potential will rise at smaller internuclear separations (except for Rydberg states of Q) than will that for the Ar^*-Q^0 intermolecular potential. Therefore, the Ar^*-Q^0 input channel cannot cross with exit channels which lie below it in energy. In the case of exit channels, including vibrationally excited states of Q*, which lie above the input channel in energy, crossing of the two curves can occur, and if the separation in energy between the two states is small, i.e., there is a small energy defect for the reaction, there is a likelihood that the crossing point of the two curves can be reached in a thermal collision. If P_x represents the probability of crossing from the input channel to the exit channel, and if $P_x \ll 1$, then σ_Q can be approximated by,[43]

$$\sigma_Q = 2\pi R_x^2 P_x \exp(\Delta E/kT),$$

where R_x is the crossing point of the two curves, ΔE is the energy defect between the curves and kT has its usual meaning. Taking $R_x = 5.5$ Å and $\Delta E = -kT$ this formula gives a quenching cross section $\sigma_a = P_x \times 70$ Å^2. Since P_x is likely to be 0.1 or less, the quenching cross sections from this model are not likely to be much larger than 10 Å^2, although cross sections as high as 30 Å^2 are possible if ΔE is small enough. Quenching by this model could lead to fairly large cross sections if the input channel were able to cross a large number of exit channels. This could occur if the coupling were into Rydberg states of the quenching molecule. Also if the input channel were coupled into a high density of vibration–rotation states of the excited quenching molecule, large cross sections might result.

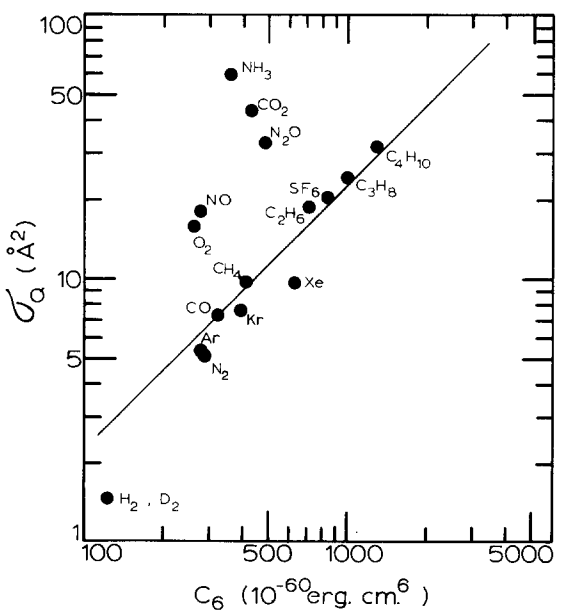

FIG. 10. The He*(2 ^3S) metastable quenching cross sections plotted against C_6. The data were taken from Ref. 56.

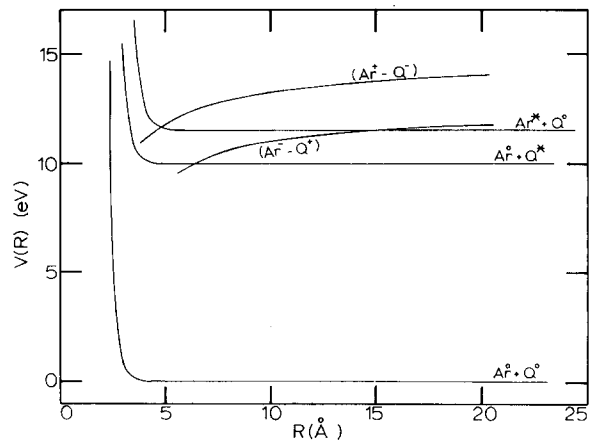

FIG. 11. Potential energy diagram for argon metastables with a general quencher Q. The Ar^*-Q^0, Ar^0-Q^*, and Ar^0-Q^0 curves are Lennard-Jones curves with σ's of 6, 4.5 and 4 Å, respectively. The C_6 coefficients have been taken to be 6.0×10^{-58} erg cm^6 for the Ar^*-Q^0 and Ar^0-Q^* curves, and 2.0×10^{-58} erg cm^6 for the Ar^0-Q^0 curve. The σ and C_6 values have been arbitrarily chosen but the relative ordering of them should be correct. The Ar^+-Q^- Coulomb curve has been calculated for E.A. (Q) = 1 eV, while Ar^-Q^+ Coulomb curve has been calculated for I.P. (Q) = 12 eV. The shape of the Ar–Q* curve should be general, but its location is arbitrary, depening on Q.

Another curve crossing possibility is to reach the exit channels through the intermediary of a charge transfer curve: Ar^+-Q^- or Ar^-Q^+.[58] In this case, the input channel crosses over onto the charge transfer curve, and is then coupled into various exit channels as the charge transfer curve crosses them. In the case of the Ar^+-Q^- curve, it is only for cases in which the quenching molecule has a large electron affinity that this channel will become likely. For example, if the electron affinity of Q is 1 eV, the charge transfer curve will cross the input channel shown in Fig. 11 ~ 0.2 eV up on the repulsive wall. Thus it is only for quenching molecules with electron affinities somewhat greater than 1 eV that this type of input channel will become inportant. One possibility which might alter this conclusion is the evaluation of $V(Ar^*-Q)$ with configuration interaction. This may serve to make the input channel more attractive for Q with E. A. $\lesssim 1.0$ eV.

It has been estimated that the electron affinity

of Ar* will be about 0.5 eV less than the excitation energy of the atom.[2a] Thus the $Ar^- - Q^+$ curve will asymptotically lie about 0.5 eV above the ionization energy of Q. The crossing of the input curve with the $(Ar^- - Q^+)$ charge transfer curve will involve an "electron jump" from Q to Ar* at the crossing point. Reasoning by analogy with the alkali halides,[59,60] this electron jump will not occur if the nuclei are separated by a large distance (> 10 Å). Thus the diabatic curves will cross, and there will not be transitions from the input channel onto the charge transfer curve. It is only for I.P. (Q) ~ 12.5 eV that the input channel crosses the $Ar^- Q^+$ curve at distances less than 10 Å and adiabatic behavior can be expected. When the ionization potential of the quenching molecule becomes greater than ~ 14 eV, the two curves cross on the repulsive wall of the input channel, so that this mechanism is again inoperative. Thus only a very few molecules should follow a charge transfer curve crossing mechanism.

We see from the above discussion that a curve crossing type of mechanism might explain large cross sections for a few special cases, such as a large density of quenching molecule states slightly endoergic with respect to the metastable energy, or a crossing of charge transfer states involving quenchers with a narrowly defined electron affinity or ionization potential. Since these conditions are not met for the bulk of quenching molecules which show large quenching cross section and a linear dependence on the C_6 coefficient, a more general quenching mechanism is sought. Presumably a curve crossing mechanism is the basic interaction for the quenching molecules with small cross sections and specific excitation channels.[2]

There has been considerable discussion recently of the long range dipole–dipole quenching mechanism.[42,46,48,50–54] In general this mechanism requires that reactants be coupled into a continuum in the product state, and that the excited atom or molecule be connected with the ground state by an optically allowed transition. For the case at hand, the first of these requirements is fulfilled, in general, since most quenchers either Penning ionize or are dissociatively excited. Weak quenchers like Kr, N_2, and CO where these product channels are not available will not concern us here. The second of the above requirements obviously does not hold since it is only magnetic quadrupole interactions that couple Ar* ($^3P_2$) to the ground state. Nevertheless this mechanism is worth considering for reasons which will become apparent. We will not go into great detail in the derivation of the mechanism, since it has been treated elsewhere.[42,46,48,50–54]

The interaction can be described by the reaction formula $A^* + Q \rightarrow A + Q'$, where Q' stands for the various excited and dissociative product states of Q. Some treatments in the literature treat cases where Q remain unexcited[52–54] and the energy is converted to some other state of A. The problem is attacked through first order time dependent perturbation theory. The rate of transitions from A* to A is given by Fermi's Golden Rule, i.e.,

$$k(t) = (2\pi/\hbar)\ \rho(E) \left| (\Psi_i\, V \Psi_f) \right|^2 , \tag{4}$$

where Ψ_i represents the initial state of $(A^* + B)$, Ψ_f the final state $(A + Q')$, $\rho(E)$ is the density of states available into which quenching may occur, and V is the interaction potential. This potential is usually given as the electric dipole terms in the multipole expansion, i.e.,

$$V = \mu_A \cdot \mu_Q / R^3 - 3(\mu_A \cdot \mathbf{R})\ (\mu_Q \cdot \mathbf{R})/R^5 \ . \tag{5}$$

Invoking the Born–Oppenheimer approximation to separate electronic and nuclear coordinates for Q and integrating the perturbation matrix element over phase space will give

$$k(t) = 2\pi/\hbar\ \rho(E)\ F_{ij}\ (M_A^2 M_Q^2)/R^6 , \tag{6}$$

where F_{ij} is the Franck–Condon factor ($F_{ij} = |(\chi_i, \chi_j)|^2$) for the molecule Q and the terms M_A^2 and M_Q^2 are the transition moments of the species and states involved, i.e.

$$M_A = (\phi_A^*\, \mu_A\, \phi_A),$$

$$M_Q = (\phi_Q\, \mu_Q\, \phi_Q),$$

where μ is the electric dipole operator. Notice that if $\phi_Q = \phi_{Q'}$ then M_Q is just the permanent dipole moment of the molecule. If Q has no dipole moment, nor states available (i.e., $Q = Q'$) then this matrix element is zero.

The probability of a transition for a given impact parameter is

$$P = \int_{-\infty}^{\infty} k(t)\, dt, \tag{7}$$

which can be integrated over a straight line trajectory[61] by setting $R(t) = (b^2 + v^2 t^2)^{1/2}$, where b is the impact parameter. This integration yields

$$P(b, v) = (\pi^2/2\hbar)\ \rho F_{ij}\ (M_A^2 M_Q^2/b^5 v) \ . \tag{8}$$

Then the quenching cross section is given by

$$\sigma(v) = \int_0^{\infty} P(b, v)\ 2\pi b\, db.$$

Notice however, that $P(b, v)$ cannot be integrated over all b since $P(b, v)$ is undefined at $b = 0$. In addition, it is unrealistic to assume a straight line trajectory for small values of b, and the multipole expansion is not valid for small distances. Thus it seems most reasonable to break the above integral into two regions:

$$\sigma(v) = \int_0^{Rc} P'(b,v) 2\pi b db + \int_{Rc}^{\infty} P(b,v) 2\pi b db, \quad (9)$$

where $P'(b,v)$ is the true probability at small impact parameters, which must be determined by other methods, and R_c is some critical impact parameter such that $P(b,v)$ given in Eq. (8) is valid for $R \geq R_c$. Putting the expression for $P(b,v)$ into the second integral in Eq. (9) and evaluating yields

$$\sigma(v) = \sigma(v)_{b<R_c} + (\pi^3/3\hbar)\, \rho F_{ij}\, (M_A^2 M_Q^2/R_c^3 v). \quad (10)$$

If we identify v with the average Boltzmann speed, $v = (8kT/\pi\mu)^{1/2}$,

$$\sigma(v) = \sigma(v)_{b<R_c} + [\pi^{7/2}/6\hbar\, (2kT)^{1/2}] \times \rho F_{ij}\, (M_A^2 M_Q^2/R_c^3)\, \mu^{1/2}, \quad (11)$$

where μ is the reduced mass of the colliding species and kT has its usual meaning. For many applications R_c has been taken as the Lennard-Jones collision diameter.

If the contributions from small impact parameters can be ignored, the quenching cross section can be parameterized as

$$\sigma_Q \propto \mu^{1/2} M_Q^2 / R_c^3 , \quad (12)$$

providing ρF_{ij} is essentially constant from one quenching molecule to another. Such a situation is likely if Q has a high density of states near the metastable energy. The transition moment, M_Q^2, can be obtained from optical measurements, e.g., photoabsorption cross sections. If relevant optical data is not available, and if M_Q^2 is integrated over all frequencies, it will be proportional to $I\alpha$, where α and I are the polarizability and ionization potential of Q. If M_Q^2 is relatively constant over a fairly wide range of frequencies, this approximation still roughly holds so that expression (12) can be given as

$$\sigma_Q \propto (\mu^{1/2} I\alpha / R_c^3). \quad (13)$$

Relation (13) is the representation of Selwyn and Steinfeld,[52] and (12) is that of Thayer and Yardley for polar quenchers.[54] There should be a certain uneasiness here with the parameter R_c since it has been arbitrarily chosen and often the total quenching cross section is of the same order of magnitude as πR_c^2, if R_c is taken as one half the sum of the Lennard-Jones diameters.

Remember that in splitting up the integral in Eq. (9) into two parts we put a restriction on R_c by requiring that $P(b,v)$ be sufficiently small that the assumptions made in its derivation be valid. If we require $P(b,v) \leq \zeta$, where ζ is some small number such that Eq. (8) holds, then

$$\zeta \geq (\pi/2\hbar)\, \rho F_{ij}\, (M_A^2 M_Q^2 / b^5 v) \quad (14)$$

or

$$b^5 \geq (\pi/2\hbar)\, \rho F_{ij}\, (M_A^2 M_Q^2/v\zeta). \quad (15)$$

The lower limit of b is R_c so that

$$R_c = [(\pi/2\hbar)\, \rho F_{ij}\, (M_A^2 M_Q^2/v\zeta)]^{1/5} . \quad (16)$$

If this value of R_c is inserted into Eq. (10) (neglecting, as before, $\sigma_b < R_c$) we get

$$\sigma(v) = (2/3)(\pi^2/\zeta^{3/5})[(\pi/2\hbar)\rho(E) F_{ij} (M_A^2 M_Q^2/v)]^{2/5}. \quad (17)$$

This $\frac{2}{5}$ dependence in the transition moment is the result derived by Förster[50] and Dexter[51] (when corrected for gas phase systems), Katsuura,[48] and Gedanken *et al.*[42] We see from this that if the dipole mechanism holds, a log–log plot of σ_Q vs $\mu^{1/2} M_Q^2$ should give a straight line with a $\frac{2}{5}$ slope. If as before M_Q^2 is identified with $I\alpha$, then a log–log plot of σ_Q vs $\mu^{1/2} I\alpha$ should also have a $\frac{2}{5}$ slope.

The implication is that the relation, $\sigma_Q \propto (\mu^{1/2} M_Q^2)^{2/5}$, should be identical to $\sigma_Q \propto \mu^{1/2} M_Q^2/R_c^3$ if the proper value of R_c is used (and R_c may not be the Lennard-Jones hard sphere collision diameter), and if $\sigma_b < R_c$ can be ignored. Since R_c cannot be known accurately, the former relation is to be preferred for correlation of data to establish the dipole–dipole mechanism. In a case where the dipole–dipole mechanism appears to fit the data, i.e., Klots $Ar^*(^1P_1)$ data,[38] both representations are *not* followed if R_c is taken as the hard sphere collision diameter; the failure of the $\mu^{1/2} M_Q^2/R_c^3$ vs σ_Q plot to have a unit slope is shown in Fig. 12, a $(\mu^{1/2} M_Q^2)^{2/5}$ vs σ_Q plot is not shown. In

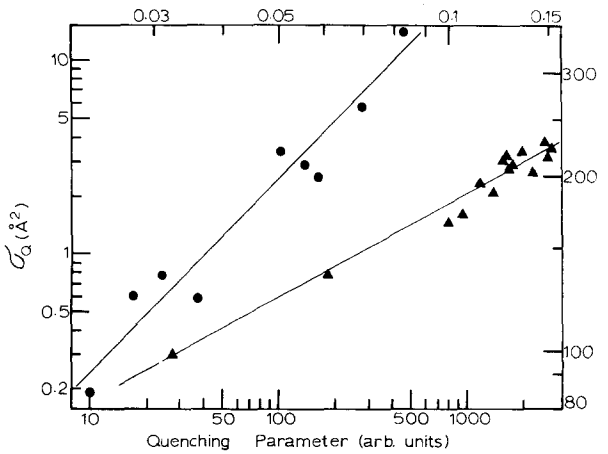

FIG. 12. I_2^* ($v' = 15$) quenching cross sections vs $\mu^{1/2} I\alpha$ (circles, left ordinate and bottom abscissa; data of Ref. 53) and $Ar^*(^1P_1)$ quenching cross sections vs $\mu^{1/2}\sigma_a/R_c^3$ (triangles, right ordinate and top obscissa; data of Ref. 38). The line through the I_2 quenching data has unit slope and that through the Ar* data has a slope of 0.53. See text for details.

a case where a unit slope correlation in the log–log plot of σ_Q vs $\mu^{1/2}I\alpha/R_c^3$ has been taken as evidence for the dipole–dipole mechanism, i.e., the iodine quenching data of Steinfeld's group,[53] a log–log plot of σ_Q vs $\mu^{1/2}I\alpha$ still has a unit slope, (see Fig. 12). Thus, doubt must be cast upon the applicability of the dipole–dipole mechanism to that system. Quenching must proceed by some other mechanism which is related to α, perhaps a dispersion interaction.[54] The dependence of argon and helium metastable quenching cross sections on α has been noted before.[8] This dependence is evident from Fig. 9 since α is the dominant factor in the calculation of C_6.

For quenching molecules whose photoabsorption cross sections, σ_a, are known[62] at the wavelength corresponding to the $^3P_2$–$^1S_0$ transition in argon, there is a general correlation with the parameters of the dipole quenching mechanism as shown in Fig. 13 by the plot of the quenching cross section vs $\mu^{1/2}\sigma_a$. Most of the data fall along a straight line of $\frac{2}{5}$ slope. Unfortunately, we cannot correlate more of our data in this manner since the pertinent photoabsorption cross sections are not known. A plot (not shown) of σ_Q vs $\mu^{1/2}I\alpha$ correlates better, in general, with a unit slope than with the $\frac{2}{5}$ slope. It is not clear, however, whether the reason is because the substitution of $I\alpha$ for σ_a, is a bad one, or because these other molecules follow a different quenching mechanism. For the cases with a known σ_a, there is a linear correlation between σ_a and α; however, there is no assurance that this is true for all of the other quenching molecules, e.g., the approximation must fail for cases with $\sigma_a = 0$ at the λ of interest.

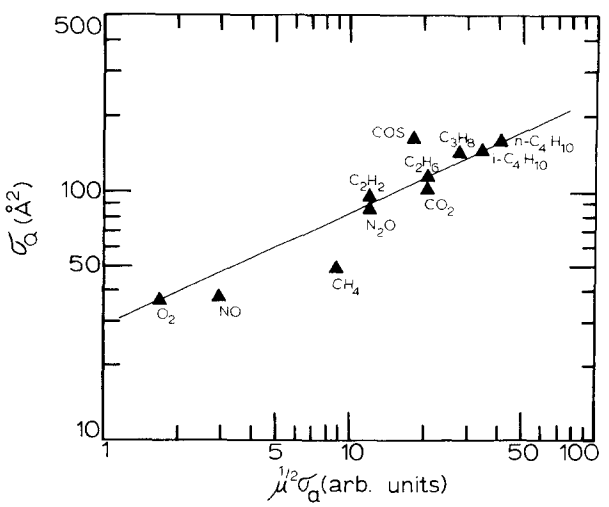

FIG. 13. Ar*($^3P_2$) metastable quenching cross sections vs $\mu^{1/2}\sigma_a$. The line drawn through the data has a slope of 2/5.

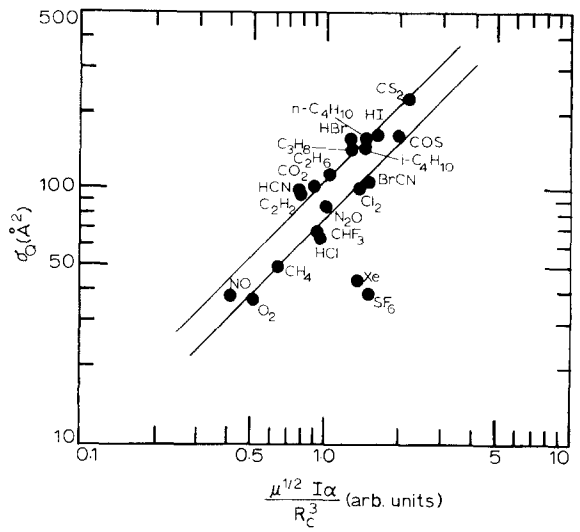

FIG. 14. Ar*($^3P_2$) metastable quenching cross sections plotted against $\mu^{1/2}I\alpha/R_c^3$. The two lines of reference are of unit slope; the data points appear to cluster about these two lines.

We also find a good correlation with the Selwyn–Steinfeld quenching parameter, although the data cluster about two lines rather than a single one, Fig. 14. As we mentioned above, the interpretation of this plot is open to some speculation. The Selwyn–Steinfeld correlation with R_c equal to the Lennard-Jones diameter, has been included for purposes of comparison, since much data have been plotted in this manner before. We do not necessarily feel that the physical model implied by the correlation is entirely correct for the quenching of argon.

The correlations shown in Figs. 9, 13, and 14 are strong evidence that the quenching mechanism is basically of a "golden rule" type, i.e., a coupling into the continuum of Q states. Presumably this coupling is similar for the various efficient molecules so that the nature of the quenching molecule essentially determines the rate of quenching. Neither the continuum of Q or the nature of the matrix element of the coupling is obvious at this time. A large variety, but not a statistical distribution, of products are observed. A reasonable guess about the exit channels is some mixture of Rydberg and dissociative states of Q. The coupling between the argon metastable and ground states is more difficult to explain. Perhaps the collision between metastable atom and quenching molecule induces a "perturbation" which removes the forbiddenness of the metastable to ground state transition. There is at least some support for this since collision induced emission has been observed at 107.3 nm in an argon discharge.[63] One would

expect, however, that the "perturbation"-induced transition moment of the metastable states would be smaller than that for the resonance states; and therefore, the resonance state quenching cross sections would be larger than those for the metastable levels, which is not the case. Another possibility is to have the collision induce a very strong mixing between the metastable and resonance states so the the metastable is essentially quenched at the same rate as the resonance states. One might expect that this mixing would be the rate determining step, but possibly it may be so strong as not to affect the quenching rate. Assuming that the data are correct, the similarity in quenching rates for $Ar(^3P_2)$ and $Ar(^3P_1)$ but the faster quenching for $Ar(^1P_1)$ creates a difficult situation to explain by simple perturbation theory. A more fruitful approach may be to retain the "golden rule" form but to formulate the matrix element in terms of the widths of the incoming channel embedded in the continuum of exit channels.[64] Clearly, further studies, both experimental and theoretical, are required before the fast quenching processes of *metastable* atoms and molecules[65] can be understood fully. It is especially desirable to have detailed comparisons of the primary products from quenching by the resonance and metastable states.

V. SUMMARY

Most of the molecules studied quench the 4*s* metastable states of argon with rates between 15 and 100×10^{-11}cm^3 molecule$^{-1}\cdot$sec^{-1}. The quenching cross section correlates linearly with C_6, the van der Waals coefficient of attraction between the metastable atom and the quenching molecule. In most cases where the photoabsorption cross section is known at wavelengths corresponding to the metastable energy, the quenching cross sections vary as $(\mu^{1/2}\sigma_a)^{2/5}$. Such a correlation has generally been taken as evidence for a dipole–dipole interaction, although in the case of argon metastables, such an interaction is forbidden to first order. In general, these correlations indicate that the quenching follows a "golden rule" rate law, although the nature of the matrix element coupling the metastable level to the ground state is open to speculation. Presumably this unknown interaction is similar for most of the molecules studied so that the nature of the quenching molecule effectively determines the magnitude of the quenching cross section. It is interesting, and not expected, that the quenching cross sections of the metastable states are similar to those for the 4*s* resonance states of argon.

ACKNOWLEDGMENTS

Financial support from the United States Army Research Office at Durham under Grant DA-AROD-31-124-71-G127 is gratefully acknowledged. We would also like to thank Dr. K. G. Kay of Kansas State University for a number of enlightening discussions.

[1]C. K. N. Patel, *Lasers*, Vol. 2, edited by Albert K. Levine (Arnold, London, 1968).
[2](a) D. H. Stedman and D. W. Setser, Prog. React. Kinet. **6**, 4 (1971). (b) J. A. Coxon, D. W. Setser, and W. H. Duewer, J. Chem. Phys. **58**, 2244 (1973). (c) G. W. Taylor, J. Phys. Chem. 77, 124 (1973). (d) D. W. Setser, D. H. Stedman, and J. A. Coxon, J. Chem. Phys. **53**, 1004 (1970). (e) D. H. Stedman and D. W. Setser, J. Chem. Phys. **52**, 3957 (1970).
[3]Robert S. Van Dyke, Charles E. Johnson, and Howard A. Shugart, Phys. Rev. A 5, 991 (1972).
[4]A. V. Phelps and J. P. Molnar, Phys. Rev. **89**, 1202 (1953).
[5]A. H. Futch and F. A. Grant, Phys. Rev. **104**, 356 (1956).
[6]E. Ellis and N. D. Twiddy, J. Phys. B 2, 1366 (1969).
[7]J. M. Anderson, Can. J. Res. **4**, 312 (1931).
[8]M. Bourène and J. Le Calvé, J. Chem. Phys. **58**, 1452 (1973).
[9]R. A. Gutcheck and E. C. Zipf, Bull. Am. Phys. Soc. **17**, 395 (1972).
[10]W. Allison, F. B. Dunning, and A. C. H. Smith, J. Phys. B **5**, 1175 (1972).
[11]L. G. Piper, W. C. Richardson, G. W. Taylor, and D. W. Setser, Discuss. Faraday Soc. **53**, 100 (1972).
[12]A. C. G. Mitchell and M. W. Zemansky, *Resonance Radiation and Excited Atoms*, (Cambridge, U. P., Cambridge, London, 1934).
[13]W. Goetz and D. A. Ramsay (private communication, 1972).
[14]E. J. Robinson, J. Levine, and B. Bederson, Phys. Rev. **146**, 95 (1966).
[15]W. L. Wiese, M. W. Smith, and B. M. Miles Natl. Stand. Ref. Data Ser. **22**, ,(1969), Vol. II.
[16]J. P. Grandin, D. Lecler, J. Margerie, C.R. Acad. Sci. (Paris) **272**, 929 (1971).
[17]E. E. Ferguson, F. C. Fehsenfeld, and A. L. Schmeltekopf in *Advances in Atomic Molecular Physics, V*, edited by D. R. Bates (Academic, New York, 1970).
[18]R. C. Bolden, R. S. Hemsworth, M. J. Shaw, and N. D. Twiddy, J. Phys. B **3**, 45 (1970).
[19]A. L. Farragher, Trans. Faraday Soc. **66**, 1411 (1970).
[20]R. W. Huggins and J. H. Cahn, J. Appl. Phys. **38**, 180 (1967).
[21]R. E. Walker, Phys. Fluids **4**, 1211 (1961).
[22]R. V. Poirer and R. W. Carr, J. Phys. Chem. **75**, 1593 (1971).
[23]M. Cher and C. S. Hollinsworth, Adv. Chem. Ser. **80**, 118 (1969).
[24]This approach has also been favored by C. L. Lin and F. Kaufman, J. Chem. Phys. **55**, 3760 (1971).
[25]J. O. Hirschfelder and M. A. Eliason, Ann. N.Y. Acad. Sci. **67**, 451 (1957).
[26](a) R. B. Bernstein and J. T. Muckerman, Adv. Chem. Phys. **12**, 477 (1967). (b) T. Nenner, D. Sc. thesis, L'Université de Paris-Sud, Centre D'Orsay, 1972, measured Lennard-Jones parameters for Ar* + Ne, Ar, Kr, Xe, N_2, D_2, and CO in a molecular beam apparatus. His results give a collision diameter for Ar* of 5.7 Å. The effect of using this lower value would be to increase the efficiency of most quenching reactions beyond unity.
[27]J. O. Hirschfelder, C. J. Curtiss, and R. B. Bird, *Molecular Theory of Gases and Liquids*, (Wiley, New York, 1954).
[28]A. Salop, E. Pollack, and B. Bederson, Phys. Rev. **124**, 1431 (1961).
[29]C. E. Moore, Circ. U.S. Natl. Bur. Stand. 467 (1949).

[30]N. T. Holcombe and F. W. Lampe, J. Chem. Phys. **56,** 1127 (1972).
[31]Z. Herman and V. Čermak, Collect. Czech. Chem. Commun. **33,** 468 (1968).
[32]H. Hotop, Diplomarbeit, Physilakisches Institut der Universität, Freiburg, Germany, December, 1967.
[33]D. H. Winicur and E. L. Knuth, Chem. Phys. Lett. **12,** 261 (1971).
[34]C. R. Lloyd, E. Weigold, P. J. O. Teubner, and S. T. Hood, J. Phys. B **5,** 1712 (1972).
[35]T. Sawada, J. E. Purcell, and A. E. S. Green, Phys. Rev. A **4,** 193 (1971).
[36]L. R. Peterson and J. E. Allen, Jr., J. Chem. Phys. **56,** 6068 (1972).
[37]I. D. Clark, A. J. Masson, and R. P. Wayne, Mol. Phys. **23,** 995 (1972).
[38]C. E. Klots, J. Chem. Phys. **56,** 124 (1972).
[39]I. P. Zapesochnyi and P. V. Feltsan, Opt. Spectrosc. **20,** 291 (1966).
[40]J. E. Parks, G. S. Hurst, T. E. Stewart, and H. L. Weidner, J. Chem. Phys. **57,** 5467 (1972).
[41]N. Thonnard and G. S. Hurst, Phys. Rev. A **5,** 1110 (1972).
[42]A. Gedanken, J. Jortner, B. Raz, and A. Szöke, J. Chem. Phys. **57,** 3456 (1972).
[43]E. H. Fink, D. Wallach, and C. B. Moore, J. Chem. Phys. **56,** 3608 (1972).
[44]C. J. Chapman, A. J. Masson, and R. P. Wayne, Mol. Phys. **23,** 979 (1972).
[45]R. J. Cross and R. G. Gordon, J. Chem. Phys. **45,** 3571 (1966).
[46]T. Watanabe and K. Katsuura, J. Chem. Phys. **47,** 800 (1967).
[47]W. R. Bennett, W. L. Faust, R. A. McFarlane, and C. K. N. Patel, Phys. Rev. Lett. **8,** 470 (1962).
[48]K. Katsuura, J. Chem. Phys. **42,** 3771 (1965).
[49]B. L. Earl, R. R. Herm, S. M. Lin, and C. A. Mims, J. Chem. Phys. **56,** 867 (1972).
[50]Th. Förster, Discuss. Faraday Soc. **27,** 7 (1959), and references therein.
[51]D. L. Dexter, J. Chem. Phys. **21,** 836 (1953).
[52]J. E. Selwyn and J..I. Steinfeld, Chem. Phys. Lett. **4,** 217 (1969).
[53]J. I. Steinfeld, Acc. Chem. Res. **3,** 313 (1970).
[54]C. A. Thayer and J. T. Yardley, J. Chem. Phys. **57,** 3992 (1972).
[55](a) K. L. Bell, A. Dalgarno, and A. E. Kingston, J. Phys. B **1,** 18 (1968). (b) We calculated C_6 using the Slater–Kirkwood approximation. The experimental results of Nenner, Ref. 26b, give a C_6 which is about a factor of 1.7 smaller than the calculated results.
[56]A. L. Schmeltakopf and F. C. Fehsenfeld, J. Chem. Phys. **53,** 2173 (1970).
[57]R. C. Bolden, R. S. Hemsworth, M. J. Shaw, and N. D. Twiddy, J. Phys. B **3,** 61 (1970).
[58]E. R. Fisher and G. K. Smith, Appl. Opt. **10,** 1803 (1971).
[59]R. S. Berry, J. Chem. Phys. **27,** 1288 (1957).
[60]J. J. Ewing, R. Milstein, and R. S. Berry, J. Chem. Phys. **54,** 1752 (1971).
[61]References 46 and 48, however, use a more sophisticated approach.
[62]R. D. Hudson, Rev. Geophys. Sp. Phys. **9,** 305 (1971), and references therein.
[63]R. C. Michaelson and A. L. Smith, Chem. Phys. Lett. **6,** 1 (1970).
[64]W. H. Miller, J. Chem. Phys. **52,** 3563 (1970).
[65]G. W. Taylor and D. W. Setser, J. Chem. Phys. 58, 4840 (1973).